Stable sums to infer high return levels of multivariate rainfall time series

Gloria Buriticá, Philippe Naveau

December 6, 2021

STABLE SUMS TO INFER HIGH RETURN LEVELS OF MULTIVARIATE RAINFALL TIME SERIES

GLORIA BURITICÁ AND PHILIPPE NAVEAU

ABSTRACT. We introduce the stable sums method for inference of extreme return levels for multivariate stationary time series. This new method is based on large deviation principles for regularly varying time series which allows for incorporation of time and space extreme dependencies in the analysis. It avoids classical declustering steps as implementation coincides for both independent and dependent observations from the stationary model. A comparison with the main estimators from extreme value theory, where detecting clustering in time is required, shows improvement of the coverage probabilities of confidence intervals obtained from our method against its competitors. Numerical experiments also point to a smaller mean squared error with the multivariate stable sums method compared to an univariate approach. We apply our method for inference of high return levels of multivariate daily fall precipitation measurements in France.

Keywords: Environmental time series; multivariate regular variation; stable distribution; stationary time series; cluster process; return levels; extremal index.

1. INTRODUCTION

Nowadays, extreme value theory [8] is frequently applied to meteorological time series to capture extremal climatological features in temperatures, winds, precipitation and other atmospheric variables [see, e.g. 30, 41, 42]. For example, due to its high societal impacts in terms of flooding, heavy rainfall have been analyzed at various spatial and temporal scales [see, e.g. 27]. In particular, storms/fronts duration and spatial coverage can produce potential temporal and spatial dependencies among recordings from nearby weather stations [see, e.g. 26]. In this multivariate context, the analysis of consecutive extremes, even in the stationary case, can be theoretically complex [see, e.g. 7, 3]. Although marginal behaviors of heavy rainfall is today well modeled, the temporal dynamic is rarely taken in account in applied studies, especially for multivariate time series [see, e.g. 20, 40, 1, 9]. To produce accurate high return level estimates from multivariate time series of extreme daily precipitation, we propose an approach to jointly incorporate the temporal dependence and the multidimensional structure among heavy rainfall. This joint modeling appears necessary to perform a full risk assessment, as ignored correlations may lead to erroneous confidence intervals. The latter is particularly important when the practitioner has to provide them about extreme occurences, i.e. interpolating beyond the largest observed value.

To contrast different climate types, we choose three stations in three different regions in France: oceanic in the northwest (Brest, Lanveoc and Quimper), Mediterranean in the south (Hyeres, Bormes-les-Mimosas and Le Luc), and continental in

northeast (Metz, Nancy and Roville). At all nine stations, recording high rainfall levels at one day is often followed by measures from rainy days latterly since an extreme weather condition can last numerous hours. This extremal dependence in time is well illustrated by the temporal extremogram[1] introduced in [12] as can be seen in Figure 1. In our case study, the multivariate aspect comes from the spatial dependence among daily rainfall measured at nearby weather stations in France from 1976 to 2015. While it is reasonable to assume independence between regions, the stations spatial proximity within a region imposes a tri-variate analysis by region. Figure 2 illustrates how high rainfall values often occur simultaneously at two close stations pointing to a strong spatial dependence of large values. Concerning seasonality, we will focus on Fall (September, October and November) as heavy rainfall have been the strongest in France during this season. Concerning marginal behaviours, records within the same region reach similar precipitation intensity levels. For example, the south of France registers higher precipitation amounts than the other two regions.

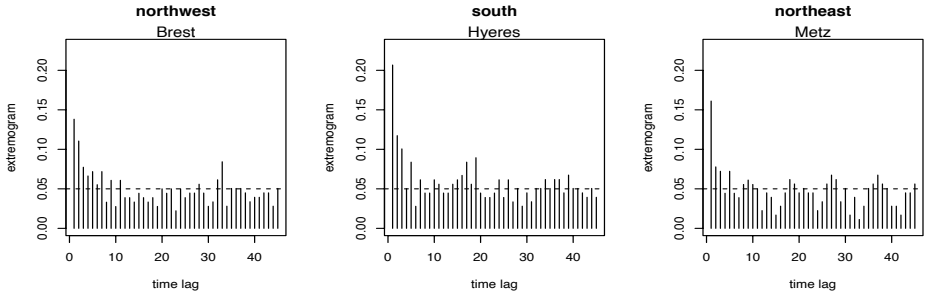

FIGURE 1. Empirical temporal extremogram of the 95-th order statistic of Fall daily rainfall from 1976 to 2015. The first, middle and last correspond to three different climatological regions in France, continental (northwest), oceanic (west) and mediterranean (south), respectively. As a baseline, the dotted line indicates the value the extremogram takes at independent time lags.

The practical goal of this study is to infer the 50 years return levels at each station, while taking in account the tri-variate dependence and the temporal memories. The theoretical added value is that we neither assume temporal independence, nor need to decluster the time series to make them independent in the upper tail. To bypass these hurdles, we build on a stable sum method. This approach takes its roots in large deviation principles and central limit theory for weakly dependent regularly varying time series [19]. In terms of notations, $(X_t)_{t\in\mathbb{Z}}$ will always represent a regularly varying stationary time series with tail index $\alpha > 0$, taking values in $\mathbb{R}^d$ that we endow with a norm $|\cdot|$, cf. [4]. In a nutshell, this means that, given large values of the norm at time zero, this norm behaves as a Pareto-type (power)

[1]The temporal extremogram is defined over time lags by $t \mapsto \lim_{x\to+\infty} pr(X_t > x \,|\, X_0 > x)$.

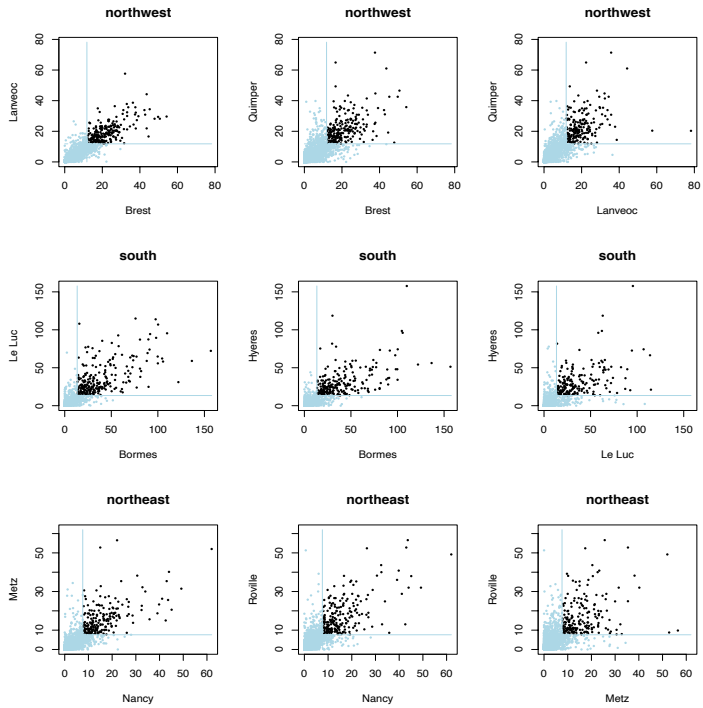

FIGURE 2. Scatter plots of Fall daily rainfall between two nearby weather stations from 1976 to 2015. The top, middle and bottom panels correspond to the three different climatological regions in France as detailed in Figure 1. Simultaneous exceedances of the 95-th order statistic of the sample $(\max\{X_t(1), X_t(2), X_t(3)\})_{t=1,\dots,n}$ are in black.

law and, for all $h \in \mathbb{N}$, it is roughly independent of $(X_t/|X_0|)_{t=-h,\dots,h}$, that contains all the dependence structure, see Equation (5) for a precise definition. In this setting, under the classical anti-clustering assumption [see e.g. 4], preventing extreme records to affect indefinitely future extremes, the following large deviation approximation holds: for any $p \geq \alpha$, $j = 1, \dots, d$,

$$pr(X_0(j) > x_n) \approx m(j)\,(n\,c(p))^{-1}\,pr\big(S_{1,n}(p) > x_n^p\big), \quad n \to +\infty, \tag{1}$$

where $S_{1,n}(p) = \sum_{t=1}^{n} |X_t|^p$ and (x_n) corresponds to a suitable sequence verifying $n\,pr(|X_0| > x_n) \to 0$ as $n \to +\infty$, $m(j)$ takes values in $[0, 1]$, for all $j = 1, \dots, d$, and $p \mapsto c(p)$ is a decreasing function. We confer to [7] the proof of (1) and its extensions[2] for $\alpha/2 < p < \alpha$.

The practical key aspect of (1) is that, whenever the constants $m(j)$ and $c(p)$ are adequately estimated, all marginal features of the multivariate vector X_0 can

[2]For $p \leq \alpha$, additional weakly mixing conditions where required in [7] to show (1). Also, for $p \leq \alpha$, $c(p) \geq 1$, and the sequence (x_n) must verify $n/x_n^{\min\{p,\alpha-\delta\}} \to 0$, for some $\delta > 0$, as $n \to +\infty$.

be easily deduced from the single univariate sum $S_{1,n}(p)$. In practice, this means that any extreme quantile of a weather station, say j, in Figure 2, can be directly deduced from the sum $S_{1,n}(p)$ computed over the group of three neighbouring stations, albeit the knowledge of the two constants $m(j)$ and $c(p)$ in (1). To interpret these two quantities, we write them as follows

(2)
$$\lim_{n\to+\infty} \frac{pr(X_0(j) > x_n)}{pr(|X_0| > x_n)} = m(j), \qquad \lim_{n\to+\infty} \frac{pr((\, S_{1,n}(p)\,)^{1/p} > x_n)}{n\, pr(|X_0| > x_n)} = c(p).$$

The ratio between the norm feature $pr(|X_0| > x_n)$ and the marginal feature $pr(X_0(j) > x_n)$ does not depend on t (as $t = 0$), and consequently, the constants $m(j)$ trace back the d-dimensional structure of extremes, but not the temporal dynamic. In contrast, the constant $c(p)$ captures the temporal clustering among extremes throughout the ℓ^p–norm. In addition, the special case of $p = \infty$ has a strong connection with the so-called declustering technique [see e.g. 23]. The constant $c(\infty)$ equals the *extremal index* of the time series $(|X_t|)_{t\in\mathbb{Z}}$, which has been interpreted as the reciprocate of the mean number of consecutive high levels to be recorded in a short period; cf. [33, 34].

A key point in our approach is to notice that the choice p in $c(p)$ is up to the practitioner. The conventional choice of taking $p = \infty$ brings the difficult problem of inferring the extremal index and finding the number of consecutive high crossings over a short time period. If we recall that [7] showed $c(\alpha) = 1$, then choosing $p = \alpha$ completely bypasses the estimation of $c(p)$. This modelling strategy obviously implies that the index of regular variation, α, needs to be estimated, a necessary step in any Pareto based quantile estimation.

The main challenge of our approach is to infer the distribution of $S_{1,n}(p)$ from the sampled multivariate vector $(X_1, \ldots, X_n)$. To reach this goal, we define the following partial sums from disjoint time periods of length b_n as

(3)
$$\underbrace{S_{1,b_n}(p)}_{:=\sum_{t=1}^{b_n}|X_t|^p}, \underbrace{S_{2,b_n}(p)}_{:=\sum_{t=b_n+1}^{2\,b_n}|X_t|^p}, \quad \cdots \quad , \underbrace{S_{\lfloor n/b_n\rfloor,b_n}(p)}_{:=\sum_{t=\lfloor n/b_n\rfloor-b_n+1}^{\lfloor n/b_n\rfloor}|X_t|^p},$$

with the convention $S_{b_n}(p) := S_{1,b_n}(p)$. The new sequence from the variables $(S_{t,b_n}(p))_{t=1,\ldots,\lfloor n/b_n\rfloor}$ provides us a transformed dataset from which the inference of $x \mapsto pr(S_{1,b_n}(p) > x)$ becomes possible. The natural question is then what is the appropriate model for $S_{b_n}(p)$. As $S_{b_n}(p)$ is a sum of regularly varying increments, then, assuming $n/b_n \to +\infty$ as $n \to +\infty$, the central limit theorem for weakly dependent stationary time series holds. More precisely, there exists positive and real sequences $(c_n(p)), (d_n(p))$ such that $(S_{b_n}(p) - d_{b_n}(p))/c_{b_n}(p)$ converges to a stable distribution with stable parameter equal to α/p, as the sums length b_n goes to infinity. Two important elements can be highlighted from this convergence. First, the family of α-stable distributions, see Section 2.1 for more detail, appears as the natural parametric family to fit the sequence $(S_{t,b_n}(p))_{t=1,\ldots,\lfloor n/b_n\rfloor}$. Second, the aforementioned choice of taking $p = \alpha$ is reinforced as the stable parameter α/p equals to one for this choice. This produces a solid yardstick to select the right

sum length b_n. In other words, an appropriate selection of b_n corresponds to the case where the distribution of $(S_{t,b_n}(\alpha))_{t=1,\dots,\lfloor n/b_n \rfloor}$ follows a stable distribution with a stable unit parameter. The algorithm behind this strategy will be explained in Section 2.3.

From a theoretical point of view, the large deviation principle in (1) is justified for inference of extreme quantiles within the scope of the sequence of threshold levels (x_{b_n}). The order of magnitude of the sequence (x_{b_n}) was studied for classical examples as linear processes in [35] and for solutions to recurrence equations in [5, 31]. For further references on large deviation probabilities for weakly dependent processes with no long-range dependence of extremes we refer to [11, 29, 28, 36]. Furthermore, central limit theory for stationary weakly dependent sequences was studied first in [11] based on weak convergence of point processes. In [29, 28] the central limit theorem was proven using classical telescopic sum arguments and large deviation limits; see [2] for a modern treatment. However, the stable domain of attraction with stable parameter equal to one has attracted little attention. Borrowing classical telescopic sum arguments, Section 5.5 provides our proof of the central limit theorem for the case with unit stable parameter, which interests us as we take $p = \alpha$. This proof will use the *cluster process* defined in [7] and has simplified assumptions compared to results in [2] and in [3].

Concerning the implementation of our stable sums method, Section 2 starts by detailing the basic ingredients of our algorithm and its main assumptions. The important step of setting the inputs of our alogrithm is explained in Section 2.3. In particular, the estimation of the stable parameter, α, is treated there. It is followed by the description of our algorithm. Our simulation study is described in Section 3. Univariate and multivariate cases are investigated. Comparisons with other approaches are implemented and commented. In Section 4, the rainfall dataset introduced with Figures 1 and 2 is analyzed in depth. The theoretical aspects of our method are detailed in Section 5.

2. Stable sums method

2.1. **Preliminaries.** Let $X := (X(1), \dots, X(d))$ be a random vector taking values in $\mathbb{R}^d$. For $T > 0$, the T–return level associated to the j-th coordinate, denoted $z_T(j)$, is defined as $z_T(j) := \inf\{z(j) : pr(X(j) > z(j)) \leq 1/T\}$. The multivariate T–return level, denoted z_T, is defined to be the $\mathbb{R}^d$-valued vector $z_T := (z_T(1), \dots, z_T(d))$. We recall below the definition and basic properties of stable distributions.

Definition 2.1. *The random variable $\xi_a := \xi_a(\sigma, \beta, \mu)$ follows a stable distribution with parameters (a, σ, β, μ) if and only if, for all $u \in \mathbb{R}$,*

(4)

$$\mathbb{E}\big[\exp\{i\,u\,\xi_a\}\big] = \begin{cases} \exp\{-\sigma^a|u|^a(1 - i\,\beta\,sign(u)\,\tan\frac{\pi a}{2}) + i\,\mu\,u\} & \text{if } a \neq 1, \\ \exp\{-\sigma|u|(1 - i\,\beta\,sign(u)\,\frac{2}{\pi}\log|u|) + i\,\mu\,u\} & \text{if } a = 1, \end{cases}$$

where $a \in (0, 2]$ is the stable parameter, $\sigma \in [0, +\infty)$ is a scale parameter, $\beta \in [-1, 1]$ is a skweness parameter, and $\mu \in \mathbb{R}$ is a location parameter.

Classical examples of stable distributions are the Gaussian distribution with $a = 2$ and $\beta = 0$, the Cauchy distribution with $a = 1$ and $\beta = 0$; and the Lévy distribution with $a = 1/2$ and $\beta = 1$. Stable distributions satisfy the reflection property: if $\xi_a := \xi_a(1, \beta, 0)$ is a stable random variable with parameters $(a, 1, \beta, 0)$, then $-\xi_a$ is a stable random variables with parameters $(a, 1, -\beta, 0)$. The stable distribution is symmetric when $\beta = 0$, and has support in $\mathbb{R}$ when $|\beta| \neq 1$. If $\beta = 1$ there are three cases: if $a < 1$ then the support of its density admits a finite lower bound. If $a = 1$ the density is supported in $\mathbb{R}$ but only the right tail is regularly varying. Otherwise, the stable distribution admits two heavy tails. A full summary on stable distributions can be found in [21, 38, 39].

2.2. **Model assumptions.** In the remaining of the article we work under the assumptions fixed here. We consider $(X_t)_{t\in\mathbb{Z}}$ to be a regularly varying time series taking values in $(\mathbb{R}^d, |\cdot|)$, with index of regular variation $\alpha > 0$; cf. [4]. This means there exists an $\mathbb{R}^d$-valued time series $(\Theta_t)_{t\in\mathbb{Z}}$ verifying $|\Theta_0| = 1$ a.s. and

$$pr((X_t)_{|t|=0,\dots,h} \in \cdot \,|\, |X_0| > x) \xrightarrow{d} pr(Y(\Theta_t)_{|t|=0,\dots,h} \in \cdot), \quad x \to +\infty, \tag{5}$$

where Y is (α)–Pareto distributed, i.e. $pr(Y > y) = y^{-\alpha}$, for all $y > 1$, independent of $(\Theta_t)_{t\in\mathbb{Z}}$. We fix $|\cdot|$ to be the supremum norm, i.e. $|X_0| := \max_{j=1,\dots,d} |X_0(j)|$, but any choice of norm is possible under minor modifications.

We also suppose that the classical conditions linked to weakly dependent regularly varying time series (see Lemma 5.2 and Proposition 5.4 in Section 5 for details) are satisfied. Then, approximation (1) holds and the renormalized process of partial sums $S_{b_n}(p)$ converges to a stable distribution with stable parameter $a = \alpha/p$ as $n \to +\infty$. Motivated by Proposition 5.4, we also set the skweness parameter $\beta = 1$ to simplify computations.

2.3. **Choice of the algorithm inputs.** To construct the time series given by the partial sums $(S_{t,b_n}(\alpha))_{t=1,\dots,\lfloor n/b_n \rfloor}$ defined by (3), we need to determine the sum length, b_n, and α. In addition, the indexes of spatial clustering $m(j)$ are required to use (1).

We estimate the index of regular variation α using the unbiased Hill estimator of [13], see their Equation (4.2) of $\widehat{\alpha}_n$ that varies in function of the order statistics k. Fixing the choice of k one obtains a point estimate[3] $\widehat{\alpha}^n = \widehat{\alpha}^n(k)$.

Concerning the inference of $m(j)$, we recall that (2) and (5) imply that

$$m(j) = \mathbb{E}[\textstyle\int_1^{+\infty} \mathbb{1}(y\,\Theta_0(j) > 1) d(-y^{-\alpha})] = \mathbb{E}[(\Theta_0(j))_+^{\alpha}],$$

where Θ_0 is an $\mathbb{R}^d$-valued random variable verifying $|\Theta_0| = 1$ a.s. For a review on inference of the spectral measure Θ_0, we refer to [7, 10, 14]. In this context, given $\widehat{\alpha}^n$, all $m(j)$ are simply estimated by the following empirical means

$$\widehat{m}^n(j) := \tfrac{1}{k} \textstyle\sum_{t=1}^n \{(X_t(j))_+^{\widehat{\alpha}^n} \,/\, |X_t|^{\widehat{\alpha}^n}\} \mathbb{1}(|X_t| \geq |X_{(k)}|), \tag{6}$$

[3]To implement Equation (4.2) as a function of the number of higher order statistics k, we set the second order parameter $\widehat{\rho} \leq 0$ to be the median value of $\widehat{\rho}(k_\rho)$ for k_ρ verifying $2 \leq k_\rho \leq k$, following the main ideas in [25, 13]. Given the trajectory $k \mapsto \widehat{\alpha}^n(k)$, we suggest to choose a point estimate from a steady portion of the plot of this trajectory.

where $j = 1, \dots, d$, $|X_{(k)}|$ is the k–th largest order statistic from the norm sample that we fix to be the 95–th empirical quantile for the remaining of this article.

To select the temporal window b_n, we recall that the renormalized partial sums, $(S_{t,b_n}(p))_{t=1,\dots,\lfloor n/b_n \rfloor}$, should follow, for $p = \alpha$, a stable distribution with stable parameter $a = 1$. So, for a given b_n, we run a ratio likelihood test for the null hypothesis $(H_0) : a = 1$ and we only keep pairs $\widehat{\alpha}^n, b_n$ such that the null hypothesis is not rejected at the 0.05 level. This heuristic allows one to discard an unsuitable choice for the couple $\widehat{\alpha}^n, b_n$. All these steps are summarized in the following algorithm.

2.4. **Algorithm.**

Algorithm 1. Stable sums estimator of the multivariate T–return level
Input: $(X_t)_{t=1,\dots,n}, b_n, \widehat{\alpha}^n, \widehat{m}^n$; see Section 2.3,
Output: $\widehat{z}^n_T$,

compute $(S_{t,b_n}(\widehat{\alpha}^n))_{t=1,\dots,\lfloor n/b_n \rfloor}$ as in (3) with $p = \widehat{\alpha}^n$,
fit stable parameters from maximum likelihood estimation: $\widehat{\theta}$,
fit stable parameters fixing $a = 1$: $\widehat{\theta}^{a=1}$,
test the null hypothesis $(H_0) : a = 1$ using ratio likelihood test,
if (H_0) is not rejected:

$$\widehat{\theta} = \widehat{\theta}^{a=1}, \tag{7}$$

if $d > 1$:
for $j = 1, \dots, d$:
calculate $q_T(j)$ as a stable quantile with parameters $\widehat{\theta}$,
evaluated at $(1 - (T\,\widehat{m}^n(j)\,)^{-1})^{b_n}$, following equation (1),
if $d = 1$:
$\widehat{m}^n(1) = 1$,
calculate $q_T(1)$ as a stable quantile with parameters $\widehat{\theta}$,
evaluated at $(1 - 1/T)^{b_n}$,

return: $\widehat{\mathbf{z}}^n_T := \big((q_T(1))^{1/\widehat{\alpha}^n}, \dots, (q_T(d))^{1/\widehat{\alpha}^n}\big)$,
else:
choose a different pair of parameters $\widehat{\alpha}^n, b_n$.

The estimated multivariate T–return level is the output of Algorithm 1 applied to $(X_t)_{t=1,\dots,n}$. If $d = 1$ then $m(1) = 1$ and both estimates coincide. Confidence intervals are obtained by sampling parametric bootstrap replicates from a stable distribution with parameters $\widehat{\theta}$, as in equation (7) from Algorithm 1. For each replicate, we evaluate a stable quantile at $(1 - (\widehat{m}^n(j)\,T)^{-1})^{b_n}$, for $j = 1, \dots, d$, and return the $1/\widehat{\alpha}^n$–power of the computed quantile. We then use the percentile bootstrap method with a significance level at 0.05 to obtain the confidence intervals. We refer to [15, 16, 17, 18] for large-sample theory of the maximum likelihood estimator for stable distributed sequences. Indeed, bounds for the derivatives of

the density function in terms of the parameters $(x; a, \sigma, \mu)$ have been computed therein; see also [37] for an overview on maximum likelihood methods for stable distributions.

3. Simulation study

3.1. **Models.** We consider the following weakly dependent regularly varying time series in our numerical experiment.

- *Burr model:* Let $(X_t)_{t=1,\dots,n}$ be independent random variables distributed as F with

$$F(x; c, \kappa) = 1 - \left(1 + x^c\right)^{-\kappa}, \quad x > 0, \tag{8}$$

  where $c, \kappa > 0$ are shape parameters. Moreover, X_1 is univariate regularly varying with index of regular variation $\alpha = \frac{1}{c\kappa} > 0$.
- *Fréchet model:* Let $(X_t)_{t=1,\dots,n}$ be independent random variables distributed as F with

$$F(x; \alpha) = e^{-x^{-\alpha}}, \quad x > 0, \tag{9}$$

  then X_1 is univariate regularly varying with tail index $\alpha > 0$.
- *ARMAX model:* Let $(X_t)_{t=1,\dots,n}$ be sampled from $(X_t)_{t\in\mathbb{Z}}$ defined as the stationary solution to the equation

$$X_t = \max\left\{\lambda\, X_{t-1}, \left(1 - \lambda^\alpha\right)^{1/\alpha} Z_t\right\}, \quad t \in \mathbb{Z}, \tag{10}$$

  where $\lambda \in [0, 1)$, and $(Z_t)_{t\in\mathbb{Z}}$ are independent identically distributed Fréchet innovations with tail index of regular variation $\alpha > 0$. Then $(X_t)_{t\in\mathbb{Z}}$ is regularly varying with same index of regular variation but with extremal index equal to $1 - \lambda^\alpha$.
- *mARMAX$_\tau$ model:* Let $(X_t)_{t=1,\dots,n}$ be sampled from $(X_t)_{t\in\mathbb{Z}}$ defined as the stationary solution to the equation

$$X_t(j) := \max\left\{\, \lambda(j) X_{t-1}(j), \left(1 - (\lambda(j))^\alpha\right)^{1/\alpha} Z_t(j)\, \right\}, \qquad t \in \mathbb{Z}, \tag{11}$$

  for $j = 1, \dots, d$, where λ takes values in $[0, 1)^d$ and $(Z_t)_{t\in\mathbb{Z}}$ are independent identically distributed vectors from a Gumbel copula with Fréchet marginals and index of regular variation $\alpha > 0$. Moreover, Z_1 is distributed as G defined by

$$G(x; \alpha, \tau) = e^{-\left((x(1))^{-(\alpha/\tau)} + (x(2))^{-(\alpha/\tau)} + \cdots + (x(d))^{-(\alpha/\tau)}\right)^\tau}, \tag{12}$$

  for $x \in \mathbb{R}^d$, and $\tau \in [0, 1]$ that we refer as the coefficient of spatial dependence. The stationary solution $(X_t)_{t\in\mathbb{Z}}$ is multivariate regularly varying with index of regular variation $\alpha > 0$; cf. [22] for more details.

  Moreover, straightforward computations from (12) yield

$$m(j) = \lim_{x\to+\infty} \frac{pr(X_0(j) > x)}{pr(|X_0| > x)} = \lim_{x\to+\infty} \frac{1 - e^{-1/x^\alpha}}{1 - e^{-d^\tau/x^\alpha}} = \frac{1}{d^\tau} < 1, \tag{13}$$

  for all $j = 1, \dots, d$. Then, from (13) we recover the symmetric properties of the Gumbel copula as $m(1) = \cdots = m(d) = 1/d^\tau$. We can also

see from (13) that the coefficient of spatial dependence $\tau \in [0,1]$ plays a key role while measuring the spatial dependence of extremes. Indeed, similar calculations allow one to compute the spatial dependence parameter between any two marginals, say $j, j\prime$, as

$$\lim_{x\to+\infty} pr(X_0(j) > x \,|\, X_0(j') > x) = 2 - 2^{\tau}, \tag{14}$$

thus $\tau = 1$ points to asymptotic independence of extremes, whereas $\tau = 0$ indicates complete dependence of extremes.

3.2. **Numerical experiment.** We perform a Monte Carlo simulation study to address two main points. Fist, we aim to compare the stable sums method with the classical methods based on declustering such as the *peaks over threshold* method, built on the generalized Pareto distribution, and the *block maxima method*, built on the generalized extreme value distribution; details are deferred to Section 3.4. Second, we aim to evaluate the relevance of the multivariate approach when compared to the univariate approach in our study.

We estimate return levels z_T for periods $T = 20, 50, 100$ years corresponding to the 99.95-th, 99.98-th and 99.99-th quantiles. We simulate 1000 trajectories of length $n = 4000$ from the models presented in Section 3.1 with parameters:

1. Burr(c, κ) model with $(c, \kappa) = (2, 2)$ in (8).
2. Fréchet(α) model with $\alpha = 4$ in (9).
3. ARMAX(λ) model with $\alpha = 4$, for both $\lambda = 0.7$ and $\lambda = 0.8$ in (10).
4. mARMAX$_\tau(\lambda)$ model taking values in $[0, +\infty)^3$ with $\alpha = 4$ and $\lambda = (0.7, 0.7, 0.7)$ in (11), and for $\tau = 0.1, 0.2, \ldots, 0.9$, in (12).

The true value is $\alpha = 4$ in all the models considered in our experiment and this corresponds to a typical rainfall tail index.

3.3. **Implementation of stable sums method.** In our simulation study we fix the index of regular variation to be $\widehat{\alpha}^n = \widehat{\alpha}^n(k)$ (see Section 2.3 for details) with $k = n^{0.7}$ for the Burr model and $k = n^{0.9}$ for the Fréchet, ARMAX and mARMAX models. Now notice that plugging in the estimates $\widehat{\alpha}^n, \widehat{m}^n$ in Algorithm 1 we can run the stable sums method as a function of the sum lengths b_n. In this way, we implement our method for the sum lengths $bl = 2^i$, with $i = 4, 5, 6, 7$. We sample $R = 100$ parametric bootstrap replicates to compute confidence intervals for the estimated return levels. For the multivariate models, we compute both the multivariate and univariate stable sums estimator.

3.4. **Implementation of classical methods.** For the univariate models, we also run the classical peaks over threshold and block maxima methods [see e.g. 8]. We address time-dependence using clusters of exceedances theory motivated by the point process approach in [11]. We refer to [7, 32] for a modern literature on this topic. A brief description of both implementation procedures is given below.

The peaks over threshold method consists in modelling the exceedances over a large threshold with a generalized Pareto distribution; see chapters 4 and 5 in [8] for an overview. In our case, we use the 95–th empirical quantile as a threshold level. Moreover, to allow for confidence intervals with larger uncertainties coming

from correlated exceedances, we consider a declustering procedure with justification in [23]. It consists of identifying clusters of exceedances as short periods with consecutive exceedances and then keeping only one from each cluster leading to a reduced sample size to fit the Pareto model. We use the code in the R-package *extRemes 2.0.12* and implement it as in the guide in [24] retaining the largest record from each cluster.

The block maxima method models the largest records obtained from disjoint vectors of consecutive observations, called blocks, with a generalized extreme value distribution; see chapters 3 and 5 in [8] for an introduction. We implement it over disjoint maxima blocks of length $bl_{BM} = 20$. However, in the time-dependent case high values might appear as clusters with consecutive large records. Then, because we only keep the largest record from each block, we tend to discard large values. To correct the bias from this procedure in time dependent data sets, we also estimate the extremal index using the interval's estimator in Ferro et al. [23], tuned with the 95–th empirical quantile. The fit of a generalized extreme value distribution, the extremal index estimation and the extrapolation is conducted using the R-package *extRemes 2.0.12*; see also the guide [24] for details.

3.5. **Simulation study in the univariate case.** The estimation of the index of regular variation, as detailed in Section 3.3, yields unbiased estimates for the Burr(2,2), Fréchet(4) and ARMAX models (plots can be available upon request).

We can see from Figure 3 that the median estimate of the 50 years return level with the peaks over threshold method underestimates the real value when implemented at the dependent models which underrates the risk. In comparison, the block maxima method is unbiased for all four models. However, it has a larger spread compared to the stable sums methods. Our method gives satisfactory results and, as expected, the choice of the sum length can be seen as a trade-off between bias and variance. We conclude that Algorithm 1 works fine coupled with a good estimate of the index of regular variation as the one detailed in Section 2.3 for both dependent and independent models.

To measure the accuracy of the confidence intervals of all methods, we compute the number of times they capture the correct value. One must keep in mind that for the stable sums method Algorithm 1 only returns an estimate if the test of the stable parameter equal to one is accepted. We summarize the sample coverage probabilities and provide the proportion of acceptance of the ratio test among the 1000 simulated trajectories from each model in Table 1. The coverage results are not reliable when the proportion of test acceptance is small, however, it increases as the sum length increases. As a result, we notice from Table 1 that we automatically discard the very small sum lengths.

To sum up, we read from Table 1 that coverage probabilities are unsatisfactory for the peaks over threshold method, specially for the models with time dependence of extremes. The coverage for the block maxima method is not well calibrated and gives poor results for the Burr model which is the only model with a marginal distribution that does not belong to the family of generalized extreme value distributions. In this manner, we aim to point at the deficiency of the classical methods

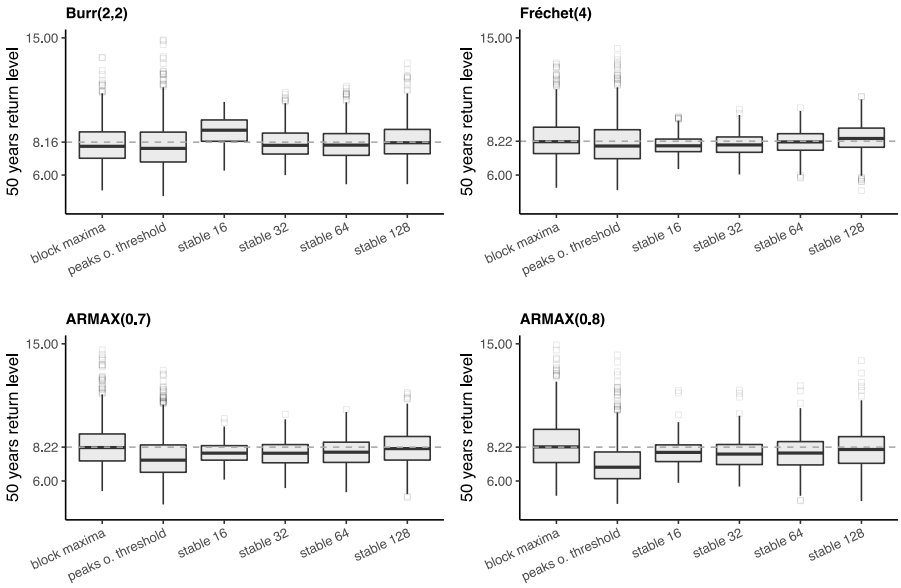

FIGURE 3. Boxplots of estimates of $\widehat{z}_T^n$ with different methods such that stable 16 refers to the stable sums method implemented for the sum length $2^4 = 16$. Dotted lines indicate the true values.

on small sample sizes. Instead, the stable sums method outperforms the block maxima and peaks over threshold methods for sum lengths between 32 and 64, where acceptance of the ratio likelihood test is significant.

3.6. **Simulation study in the multivariate case.** We inquiry now the performance of the multivariate, as opposed the univariate, stable sums estimator as we aim to capture the spatial features of extremes. We compute both estimates for the samples from the mARMAX$_\tau$ model with $\lambda = (0.7, 0.7, 0.7)$ as in (11); see Section 3.2 for details. We compare the performance of both estimators at each coordinate, $j = 1, 2, 3$, in terms of the relative percentage change of the mean squared error. More precisely, for each coordinate, we compute the mean squared error of the multivariate and univariate estimates denoted MSE_{MV} and MSE_{UV}, respectively, and relate them through the equation

$$\text{relative percentage change of MSE} \;=\; \frac{MSE_{UV} - MSE_{MV}}{MSE_{UV}} \times 100. \tag{15}$$

We also compute the relative percentage change of the squared variance, and of the absolute bias, from equations similar to (15). Large positive values point to an improvement of the multivariate estimator, while negative values detect a deterioration of its performance.

We omit details on coverage probabilities as both estimator have similar coverage as the ARMAX(0.7) univariate model (as expected due to the relation in (11)). We detail only the analysis on the third coordinate for estimates $z_T(3)$ of

		years				years		
		20	50	100		20	50	100
		coverage				coverage		
	Burr(2,2)				Fréchet(4)			
block maxima		.91	.89	.87		.93	.93	.92
peaks o. threshold		.87	.85	.83		.89	.87	.86
stable 16	(.06)	.89	.85	.80	(.53)	.94	.95	.95
stable 32	(.51)	**.93**	**.94**	**.95**	(.83)	**.96**	**.96**	**.96**
stable 64	(.85)	**.95**	**.95**	**.97**	(.90)	.96	.99	.99
stable 128	(.94)	.87	.98	.98	(.91)	.82	.99	.99
	Armax(0.7)				Armax(0.8)			
block maxima		.93	.93	.92		.92	.91	.91
peaks o. threshold		.78	.79	.79		.66	.72	.74
stable 16	(.21)	.92	.94	.93	(.12)	.80	.82	.84
stable 32	(.66)	.90	.90	.91	(.55)	.87	.89	.90
stable 64	(.89)	**.93**	**.96**	**.96**	(.85)	**.90**	**.93**	**.93**
stable 128	(.94)	.85	.97	.98	(.92)	.83	.95	.96

TABLE 1. The sub-index in parenthesis indicates the proportion of acceptance of the ratio test $(H_0) : a = 1$. In bold we highlight the optimal choice of sum length for the stable sums method. In our study, a precise coverage should be at 0.95.

the $T = 50$ years return level, similar results hold over all coordinates and can be available upon request. The relative percentage changes are plotted in figure 4 as a function of the spatial dependence coefficient τ. We notice that for the sum lengths 32 and 64, the multivariate outperforms the univariate estimator. Indeed, the choice of sum length 64 was optimal for the ARMAX(0.7) univariate model as pointed out by Table 1.

Moreover, for values of τ close to 0.5, the multivariate estimator has an outstanding improvement, mainly due to a diminution of bias. As τ approaches 1, and the model approaches the regime of asymptotic independence, the multivariate also outperforms the univariate estimator though the choice of sum length becomes delicate. In contrast, the amelioration is less evident for values of τ close to 0. Recall from equation (14) that $\tau = 0$ points to asymptotic dependence and thus $m(j) = 1/d^{\tau} = 1$ can be difficult to estimate. We conclude that in general the multivariate estimator is preferable to the univariate approach. However, there is a need for future work to identify, both theoretically and practically, which are the features on the space dependence structure pointing to an overall improvement of the multivariate inference procedures for extremes.

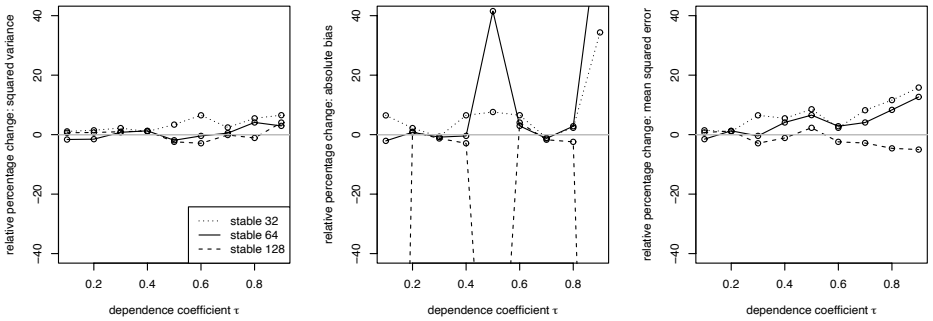

FIGURE 4. Relative percentage change of the multivariate against the univariate estimator (for the 50 years return level $z_T(3)$ estimator) of the: squared variance, absolute bias and mean squared error as in (15), from left to right.

4. CASE STUDY: HEAVY RAINFALL IN THE THREE FRENCH REGIONS

We recall the data set of daily rainfall amounts introduced in Section 1 and our goal of computing the expected level of daily rain to be exceeded in the next 50 years at all the nine weather stations in France. We conduct our analysis separately over the three different regions: northwest, south, and northeast of France. We apply our method at each region using the Fall measurements from the three nearby weather stations. Mainly, fall observations from the same region are modelled as a 3-dimensional sample $(X_t)_{t=1,\dots,n}$ from a stationary multivariate regularly varying time series denoted $X_t := (X_t(1), X_t(2), X_t(3))$, $t \in \mathbb{Z}$. We include both wet and dry days in our daily observations. In this setting, our goal of estimating the expected daily precipitation record to be exceeded in the next 50 years at each station in the Fall traduces to estimating the 99.98-th quantile of $X_0(j)$, for $j = 1, 2, 3$.

4.1. **Implementation.** To study the samples $(X_t)_{t=1,\dots,n}$ obtained from each region, we implement the stable sums method as a function of the number of order statistics k in the following way. For $k = 150, 250, 350, 450, 550$, first we compute estimates $\widehat{\alpha}^n(k)$ as described in Section 2.3. Then, for each estimate we search the sum length larger than 32 for which the $p-$value of the ratio likelihood test from Algorithm 1 is minimized. We look only among the sum lengths from the first 20 acceptances of the test. For comparison, we also implement classical methods as a function of the number of order statistics k as follows: we compute the peaks over threshold method for threshold levels $th(k) = X_{(k)}$ such that $X_{(1)} \geq X_{(2)} \geq \cdots \geq X_{(n)}$, and we compute the block maxima method for blocks of length $bl_{BM}(k) := n/k$.

4.2. **Analysis of the radial component.** At each region, we start by studying the supremum norm observations, i.e. $(|X_t|)_{t=1,\dots,n}$. We apply all three methods to

estimate confidence intervals for the 50 years return level of Fall observations of the supremum norm. The obtained estimates are presented in Figure 5 where the rows correspond to different regions and the columns correspond to different methods. We notice that, as suggested by the simulation study in Section 3, the confidence intervals obtained with the peaks over threshold method might be too narrow and underestimate the expected return level. We also remark that the block maxima method varies strongly for different block length choices in Figure 5, thus a careful choice is required. Finally, we conclude that the stable sums method, illustrated in the third column of Figure 5, gives robust estimates as a function of k.

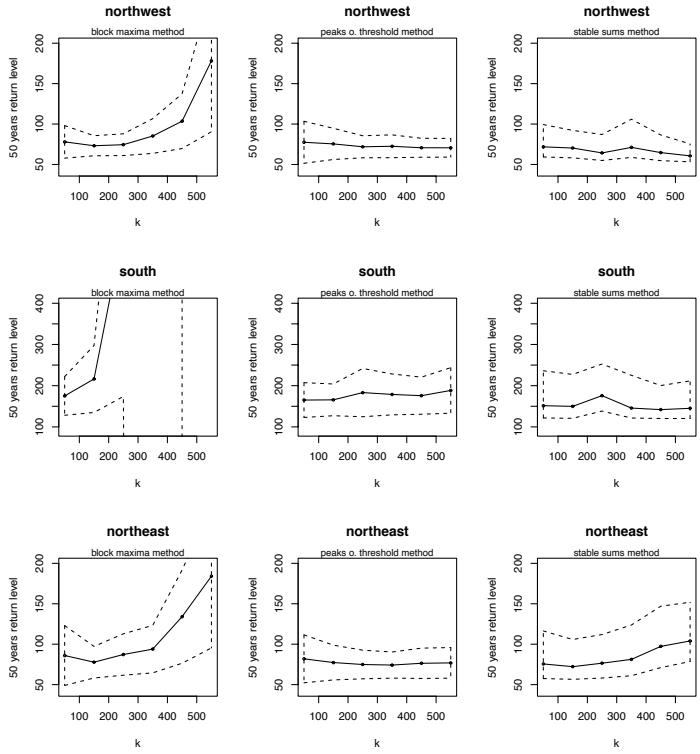

FIGURE 5. Estimates of the 50 years return level of Fall observations of the supremum norm with confidence intervals. We write estimates as a function of k with the parametrization described in Section 4.1.

To complete the analysis on the supremum norms we look at qqplots of the observed records $(S_{i,bl}(\widehat{\alpha}^n(k))^{1/\widehat{\alpha}^n(k)})_{i=1,\dots,\lfloor n/bl \rfloor}$ against the theoretical stable quantiles to the power $1/\widehat{\alpha}^n(k)$, for $k = 150, 250, 350, 450$, where sum lengths are chosen as detailed in Section 4.1. Figures 6, 7, 8 contain the qqplots for the northwest, south and northeast, respectively, and allow us to assess goodness of fit for the different choices of k. We conclude from Figure 6 that for the northwest locations, the choice $k = 350$, $bl = 165$ captures nicely the intermediate and extreme

quantiles. For the southern region, we see in Figure 7 that the choice $k = 250$ and $bl = 105$ gives an accurate fit. Lastly, for the northeast region, Figure 8 suggests the choices $k = 350$ and $bl = 70$, or $k = 450$ and $bl = 53$, for a correct alignment of intermediate and high quantiles.

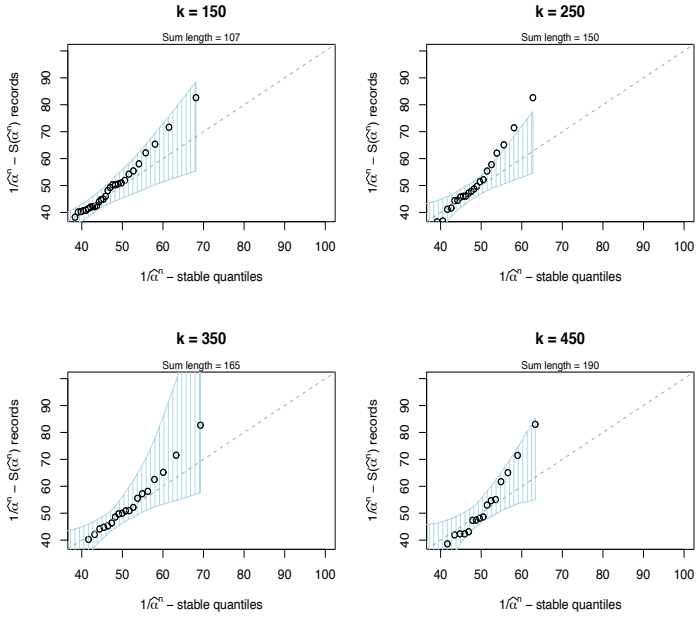

FIGURE 6. qqplots for different k values of the $1/\widehat{\alpha}^n(k)$–stable quantiles against the $1/\widehat{\alpha}^n(k)$–$(S_{t,b}(\widehat{\alpha}^n(k)))_{t=1,\ldots,\lfloor n/b \rfloor}$ records with 95% confidence intervals for the northwest.

To summarize, the stable sums method is robust for different choices of k and qqplots allow one to assess goodness-of-fit properties.

4.3. **Analysis of the multivariate components.** Finally, we come back to the question of computing the expected daily rainfall record to be exceeded in the next 50 years in the Fall at each station. In this case, we also estimate the indexes of spatial clustering. Relying on (6) we obtain estimates: $\widehat{m}^n = (0.4966, 0.2709, 0.5744)$ corresponding to the weather stations at Brest, Lanveoc and Quimper in the northwest region; $\widehat{m}^n = (0.6064, 0.4706, 0.2866)$ for Bormes, Le Luc and Hyeres in the south; and $\widehat{m}^n = (0.3910, 0.4448, 0.5649)$ for Nancy, Metz, Roville in the northwest.

Roughly speaking, we can interpret (1) to say: high daily rainfall levels at each weather station can be modelled as high quantiles from a stable distribution. In particular, by letting the largest order statistics from each station play the role of the sequence of high threshold levels in (1), we deduce an empirical version of this relation which can be rewritten as

$$pr((S_{b_n}(\widehat{\alpha}^n))^{1/\widehat{\alpha}^n} \leq X_{(k)}(j)) \;\approx\; 1 - \frac{k}{\widehat{m}^n(j)\, n/b_n}\,, \tag{16}$$

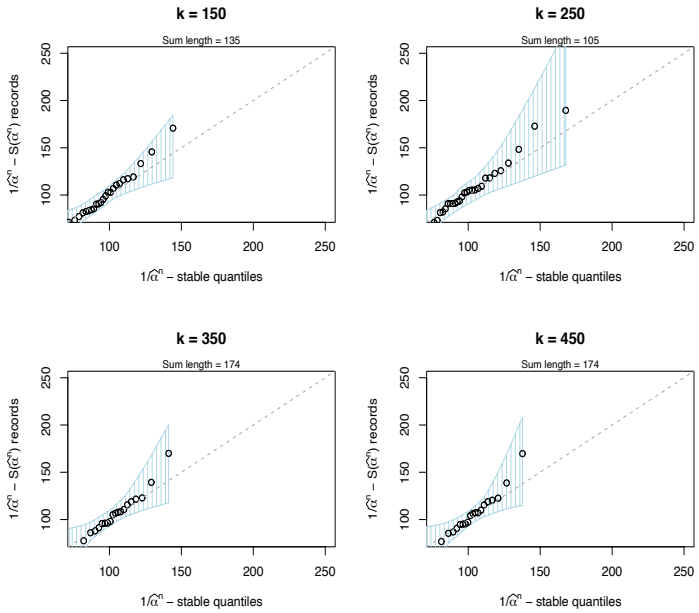

FIGURE 7. qqplots for different k values as in Figure 6 but for the southern region.

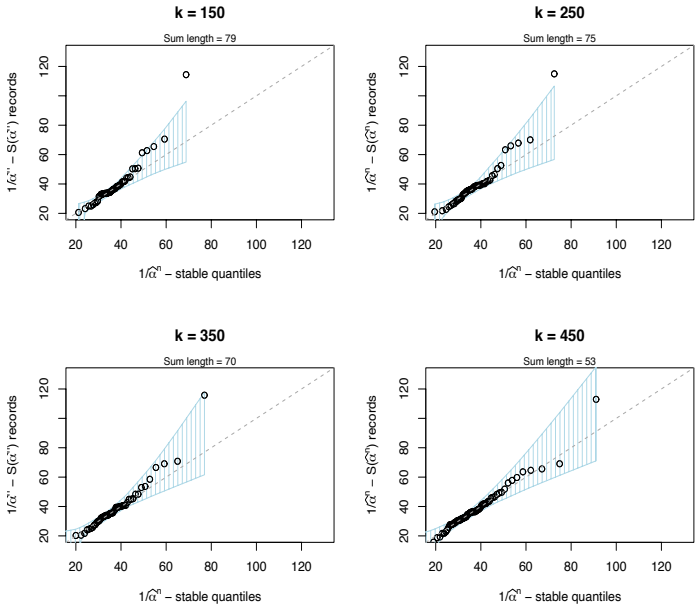

FIGURE 8. qqplots for different k values as as in Figure 6 but for the northeast region.

where $X_{(1)}(j) \geq X_{(2)}(j) \geq \cdots \geq X_{(\lfloor n/b_n \rfloor)}(j)$, for $j = 1, \ldots, d$. However, the approximation in (16) is only justified for the largest observations recorded. Moreover, the left-hand side in (16) can be approximated from the stable distribution fitted in (7) in Algorithm 1.

In this way, we inspect equation (16) by plotting the sample largest order statistics $(X_{(t)}(j))_{t=1,\ldots,\lfloor \widehat{m}^n(j) n/b_n \rfloor}$, against the $1/\widehat{\alpha}^n$–stable quantiles from the distribution fitted at (7) in Algorithm 1 for the multivariate stable sums method. For comparison with the univariate approach, we also plot the largest order statistics against the $1/\widehat{\alpha}^n$–stable quantiles from the univariate implementation as the following relation is also justified from (1)

$$pr((\textstyle\sum_{t=1}^{b_n}(X_t(j))^{\widehat{\alpha}^n(k)})^{1/\widehat{\alpha}^n} \leq X_{(k)}(j)) \;\approx\; 1 - \frac{k}{n/b_n}\,. \tag{17}$$

The plots are displayed in Figure 9 with points in black and grey for the multivariate and univariate approach, respectively. We use the estimates $\widehat{m}^n$, presented at the beginning of this section, and the tuning parameters $\widehat{\alpha}^n, bl$ from Section 4.2, pointing to a nice fit of the radial component. In particular, we set $k = 350$, $bl = 165$ for the northwest region, $k = 250$, $bl = 105$ for the south and $k = 350$, $bl = 70$ for the northeast. We interpret the largest records close to the diagonal as a nice fit. We remark from Figure 9 that overall the plots from the multivariate approach in black describe more accurately the most extreme observations compared to the univariate approach in grey. In particular, we can see a big improvement in the northeast region. For this region we also use the visual tool of Figure 9 to discard the choice of parameters $k = 450$ and $bl = 53$ as we found the fit from Figure 9 to be more accurate.

Moreover, the intermediate quantiles shouldn't necessarily align, and in practice, there is not a clear procedure for knowing how many of the top quantiles should line up with the diagonal. Furthermore, we notice the observations are limited when the estimates of the spatial index: $m(j)$, are close to zero and then the graphical analysis is less reliable than for values of it close to one; see e.g. the stations of Lanveoc and Hyeres. We conclude that the multivariate method captures accurately the highest rainfall records, and supported by the numerical results from Section 3.6, it is justified for addressing the spatial dependencies of extremes.

5. Asymptotic theory

5.1. **Anti-clustering condition.** In the remaining sections we provide a theoretical background to justify the stable sums method. Let $(X_t)_{t\in\mathbb{Z}}$ be a regularly varying time series taking values in $(\mathbb{R}^d, |\cdot|)$. We work under the anti-clustering condition below tailored to avoid long-range dependence of extremes. Similar conditions have also be considered in [4, 6].

Anti-clustering condition: There exists a non-negative sequence (x_n) such that for all $\epsilon > 0$,

$$\lim_{l\to+\infty} \limsup_{n\to+\infty} pr\big(\max_{t=1,\ldots,n} |X_t| > \epsilon\, x_n \,\big|\, |X_0| > \epsilon\, x_n\big) = 0, \tag{18}$$

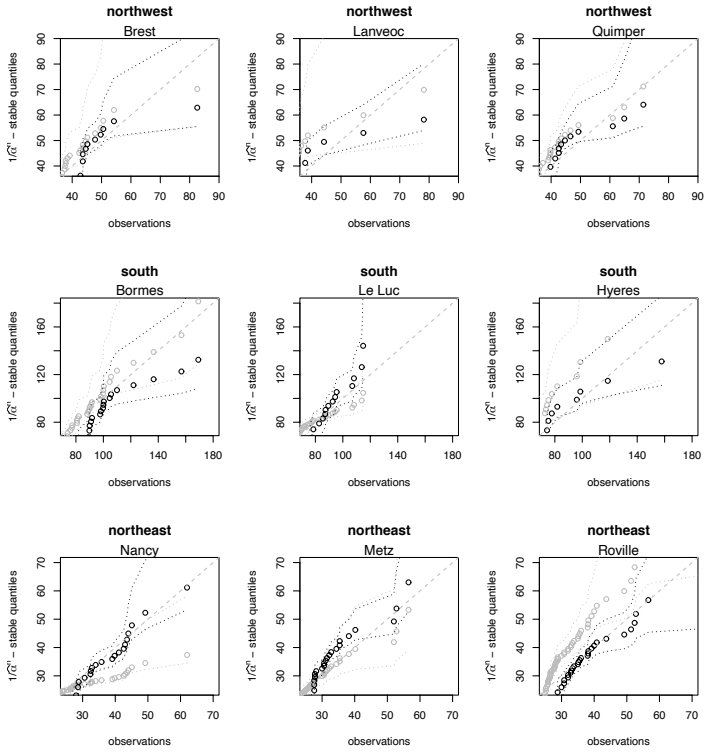

FIGURE 9. Plot of observations against the $1/\widehat{\alpha}^n$ stable quantiles for the multivariate estimator in black; see (16), and for the univariate estimator in grey; see (17), with confidence intervals. The dotted line is the identity map $x \mapsto x$.

and $n\, pr(|X_0| > x_n) \to 0$ as $n \to +\infty$.

Recall the limit time series $(\Theta_t)_{t\in\mathbb{Z}}$ from the definition of regular variation in (5). We refer to it as the spectral tail process; cf. [4], and remember it is informative of the space and time dependence of extremes for fixed windows of time. Assuming (18) entails $\|\Theta_t\|_\alpha^\alpha := \sum_{t\in\mathbb{Z}} |\boldsymbol{\Theta}_t|^\alpha < +\infty$ a.s. In this case, the overall asymptotic dependencies of the extremes of the time series are captured by the cluster process $(\Theta_t/\|\Theta\|_\alpha)_{t\in\mathbb{Z}}$ introduced in [7]. We review below this result recalling Proposition 3.2 in [7].

Lemma 5.1. *Let $(X_t)_{t\in\mathbb{Z}}$ be a time series in $(\mathbb{R}^d, |\cdot|)$ verifying regular variation as in (5), with index of regular variation $\alpha > 0$ and spectral tail process $(\Theta_t)_{t\in\mathbb{Z}}$. Then, the anti-clustering condition in (18) implies $\|\Theta_t\|_\alpha^\alpha < +\infty$ a.s. and the cluster process $(Q_t)_{t\in\mathbb{Z}}$ is well defined by the a.s. relation: for all $t \in \mathbb{Z}$, $Q_t := \Theta_t/\|\Theta_t\|_\alpha$.*

Condition (18) is also typical to justify the declustering procedures; [see e.g. 23]. For example, it grants the existence of a *extremal index* $\theta \in [0, 1]$, associated to the univariate stationary time series $(X_t)_{t\in\mathbb{Z}}$, such that for any sequence $(a_n(\kappa))$

verifying $n\,pr(|X_0| > a_n(\kappa)) \to \kappa$

$$\lim_{n\to+\infty} pr\big(\max_{t=1,\dots,n} |X_t| \le a_n(\kappa)\big) \;=\; e^{-\kappa\,\theta}. \tag{19}$$

Moreover, under (18), $\theta \in (0,1]$ and the relation $\theta = c(\infty) = \mathbb{E}[\max_{t\in\mathbb{Z}} |Q_t|^\alpha]$ holds; see [6].

5.2. **Vanishing small values condition.** In our case we aim to study the partial sums of p-powers. We require an additional assumption to deal with the sums of small or non extremal values. Assumptions of this type are typical while studying partial sums and similar versions of (20) below where also considered in [2, 11, 36, 7].

Vanishing small values condition: There exists a sequence (x_n) verifying (18), $n/x_n^{\alpha-\kappa} \to 0$, as $n \to \infty$ for some $\kappa > 0$, and for all $\delta > 0$

$$\lim_{\epsilon\downarrow 0} \limsup_{n\to+\infty} \frac{pr\big(\sum_{t=1}^n |X_t|^\alpha \mathbb{1}_{\{|X_t|\le \epsilon\, x_n\}} > \delta\, x_n^\alpha\big)}{n\,pr(|X_0| > x_n)} = 0. \tag{20}$$

Since $n/x_n^{\alpha-\kappa} \to 0$ for some $\kappa > 0$ in (20), then $n\mathbb{E}[|X_0/x_n|^\alpha \mathbb{1}_{\{|X_0|\le x_n\}}] \to 0$, which implies $S_n(\alpha)/x_n^\alpha \xrightarrow{\mathbb{P}} 0$ as $n \to +\infty$. Hence,

$$\begin{aligned}
&\frac{pr\big(\sum_{t=1}^n |X_t|^\alpha \mathbb{1}_{\{|X_t|\le \epsilon\, x_n\}} > \delta\, x_n^\alpha\big)}{n\,pr(|X_0| > x_n)} \\
&\le \delta^{-1}\, \frac{var\big(\sum_{t=1}^n |X_t/x_n|^\alpha \mathbb{1}_{\{|X_t|\le \epsilon\, x_n\}}\big)}{n\,pr(|X_0| > x_n)} \\
&\le \delta^{-1}\, \frac{\mathbb{E}\big[|X/x_n|^{2\alpha} \mathbb{1}_{\{|X_0|\le \epsilon\, x_n\}}\big]}{pr(|X_0| > x_n)} \big(1 + \textstyle\sum_{t=1}^n \rho_t\big),
\end{aligned}$$

where $\rho_t \in [0,1]$ is a correlation coefficient defined as

$$\rho_t := corr\big(|X_0|^{\alpha-\kappa}, |X_t|^{\alpha-\kappa}\big),$$

for some $\kappa > 0$. If $\sum_{t=1}^\infty \rho_t < +\infty$, then an application of Karamata's theorem yields an asymptotic upper bound given by $\delta^{-1}\,\epsilon^\alpha(1 + \sum_{t=1}^{+\infty} \rho_t)$ and (20) holds by letting $\epsilon \downarrow 0$.

5.3. **Large deviation principle.** In this section we verify the constant $c(p)$ defined in (1) satisfies $c(p) = 1$ for $p = \alpha$, the index of regular variation, under the aforementioned conditions. We review Lemma 4.1 in [7] to justify the right-hand side of (2) for the case $p = \alpha$. The proof is postponed to Section 5.5.

Lemma 5.2. *Let $(X_t)_{t\in\mathbb{Z}}$ be an $\mathbb{R}^d$–valued regularly varying time series with index of regular variation $\alpha > 0$. Assume it verifies conditions (18) and (20) for a sequence (x_n). Then*

$$\lim_{n\to+\infty} \frac{pr\big(S_n(\alpha) > x_n^\alpha\big)}{n\,pr(|X_0| > x_n)} = 1, \quad n \to +\infty. \tag{21}$$

Therefore, we interpret the choice $p = \alpha$ in (1) as a new declustering procedure that we deduce from the invariance property in (21). Indeed, the unit limit holds regardless of the underlying time dependence dynamic of extremes for numerous examples verifying (18) and (20) [see e.g. 4, 5, 36].

5.4. **Mixing condition.** In this section we verify the central limit theorem for partial sums of p-powers.We detail the case $p = \alpha$ as for $p \in (0,1) \cup (1,2)$ we refer to Proposition 5.4. in [7]. We assume also the mixing condition below holds for the time series of α-powers. We have written it using the characteristic functions of the partial sums and thus it resembles condition (2.8) in [2].

Mixing condition: Let $(Z_t)_{t\in\mathbb{Z}}$ be an $\mathbb{R}^d$–valued regularly varying time series with index of regular variation equal to one. Assume for all $\epsilon > 0$, $u \in \mathbb{R}^d$, there exists an integer sequence $k := k_n \to \infty$, verifying $n/k_n \to \infty$ and

$$\left|\mathbb{E}\left[\exp\left\{i\,u\sum_{t=1}^{n} Z_t/c_n\right\}\right] - \mathbb{E}\left[\exp\left\{i\,u\,\sum_{t=1}^{k} Z_t/c_n\right\}\right]^{\lfloor n/k\rfloor}\right| \to 0\,, \quad n \to +\infty. \tag{22}$$

where (c_n) satisfies $n\,pr(|Z_0| > c_n) \to 1$ as $n \to +\infty$.

Recall the mixing coefficients (α_t) defined, for all $h \in \mathbb{N}$, as

$$\alpha_h := \sup_{A\in\sigma\left((X_t)_{t\le 0}\right), B\in\sigma\left((X_t)_{t\ge h}\right)} |pr(A\cap B) - pr(A)pr(B)|,$$

Then, the mixing condition in (22) holds for mixing process verifying $\alpha_t \to 0$, $t \to +\infty$, using Lemma 3.8. in [2] by assuming the decay of the α-mixing coefficients happens sufficiently fast.

5.5. **Central limit theorem.** We state in Theorem 5.3 a central limit theorem for regularly varying time series with index of regular variation one. In the remaining sections we assume the conditions (22), (18), (20) hold simultaneously; see Remark 5.5. In our proof we relax the assumption (4.10) in [3] and assumption (**CT**) in Theorem 3.1. [2] for the recentering term. The proof is deferred to Section 5.5.

Theorem 5.3. *Let $(Z_t)_{t\in\mathbb{Z}}$ be an $\mathbb{R}^d$–valued regularly varying time series with index of regular variation equal to one. Let (c_n), (d_n) be sequences verifying $n\,pr(|Z| > c_n) \sim 1$ as $n \to +\infty$ and $d_n := \mathbb{E}[Z_t \mathbb{1}(|Z_t| \le c_n)]$ and assume (22), (18), (20) hold simultaneously. Then, for all $u \in \mathbb{R}^d$,*

$$\lim_{n\to+\infty} \log \mathbb{E}\left[\exp\left\{iu\textstyle\sum_{t=1}^{n}(Z_t - d_n)/c_n\right\}\right]$$
$$= \int_0^\infty \mathbb{E}\left[\exp\left\{iu\textstyle\sum_{t\in\mathbb{Z}} yQ_t^Z\right\} - 1 - i\sin\left(t\textstyle\sum_{t\in\mathbb{Z}} yQ_t^Z\right)\right] d(-y^{-1}) + i\mu(u)\,, \tag{23}$$

where the last term in (23) is a location parameter given by

$$\mu(u) := \int_1^\infty \mathbb{E}\left[\sin\left(u\textstyle\sum_{t\in\mathbb{Z}} yQ_t^Z\right) - \sin\left(u\textstyle\sum_{t\in\mathbb{Z}} yQ_t^Z - u\sum_{t\in\mathbb{Z}} \underline{yQ_t^Z}_{-1}\right)\right] d(-y^{-1}),$$

and $(Q_t^Z)_{t\in\mathbb{Z}}$ *refers to the cluster process of* $(Z_t)_{t\in\mathbb{Z}}$ *as defined in Lemma 5.1 verifying* $\|Q_t^Z\|_1 = 1$ *a.s. In particular,* $\sum_{t=1}^n (Z_t - d_n)/c_n$ *converges in distribution to a stable distribution* ξ_1 *with stable parameter one.*

Finally, from Theorem 5.3, the Proposition 5.4 below follows straightforward. The proof is presented below.

Proposition 5.4. *Let* (X_t) *be an* $\mathbb{R}^d$*–valued regularly varying time series with index of regular variation equal to* $\alpha > 0$*. Let* $(c_n(\alpha))$*,* $(d_n(\alpha))$*, be sequences verifying* $n\, pr(|X|^\alpha > c_n) \sim 1$ *as* $n \to \infty$*, and* $d_n(\alpha) := \mathbb{E}[|X_t|^\alpha \mathbb{1}(|X_t|^\alpha \le c_n)]$*. If* $(|X_t|^\alpha)_{t\in\mathbb{Z}}$ *verifies conditions (22), (18), (20) simultaneously then* $(S_n(\alpha) - d_n(\alpha))/c_n(\alpha)$ *converges in distribution to a stable random variable* ξ_1 *with stable parameter* $a = 1$ *and skweness parameter* $\beta = 1$*, as* $n \to +\infty$*.*

Proof. Let's denote by $(Q_t)_{t\in\mathbb{Z}}$ the cluster process of $(X_t)_{t\in\mathbb{Z}}$ verifying $\|Q_t\|_\alpha = 1$ a.s. We define the regularly varying time series $(Z_t)_{t\in\mathbb{Z}}$ by $Z_t := |X_t|^\alpha$ which has spectral tail process $(Q_t^Z)_{t\in\mathbb{Z}}$ equal to $Q_t^Z := |Q_t|^\alpha$, for all $t \in \mathbb{Z}$, a.s., and verifies $\sum_{t=1} Q_t^Z = 1$ a.s.

Theorem 5.3 entails $\sum_{t=1}^n (|X_t|^\alpha - d_n(\alpha))/c_n(\alpha)$ converges in distribution to a random variable ξ_1 admitting a log-characteristic function verifying for all $u \in \mathbb{R}$,

$$\log \mathbb{E}[\exp\{i\, u\, \xi_1\}] \;= \int_0^\infty \mathbb{E}\big[\exp\big\{i\, uy\big\} - 1 - i\sin(uy)\big] d(-y^{-1}) + i\mu(u)\,.$$

Then, following the lines of the argument in section XVII.2 of [21], we deduce the skweness parameter of the stable limit ξ_1 verifies $\beta = 1$. □

Remark 5.5. *In Theorem 5.3 we assume conditions (22), (18) and (20) hold simultaneously. By this we mean there exists an integer sequence* $k := k_n \to \infty$ *such that (22) holds and conditions (18) and (20) then hold for the sequence* (x_n) *defined as* $x_{k_n} := c_n$*, and* (c_n) *satisfies* $n\, pr(|Z_0| > c_n) \to 1$ *as* $n \to \infty$*. Naturally, conditions (18) and (20) are meant to study the large deviations of the vector* $(X_t)_{t=1,\dots,n}$ *as* (x_n) *needs to satisfy* $n\, pr(|X_0| > x_n) \to 0$ *as* $n \to \infty$*. Indeed, we verify*

$$k_n\, pr(|X_0| > x_{k_n}) = k_n/n\, (n\, pr(|X_0| > c_n)) \sim k_n/n \to 0$$

as $n \to \infty$*.*

Proposition 5.4 together with Lemma 5.2 justifies the model assumptions in Section 2.2. Therefore, conditions (22), (18) and (20) are sufficient to justify the Algorithm 1 built on the partial sums of $\alpha-$powers. These conditions have been demonstrated previously on numerous examples under weakly mixing assumptions; cf. [2, 36] and references therein. We conclude Section 5 demonstrates a solid theoretical background to sustain the stable sums method we proposed.

ACKNOWLEDGEMENT

The authors would like to thank John Nolan for kindly providing us with the Stable software and Olivier Wintenberger for discussions on the topic. Part of this work was supported by the DAMOCLES-COST-ACTION on compound events, the French national program (FRAISE-LEFE/INSU and 80 PRIME CNRS-INSU),

and the European H2020 XAIDA (Grant agreement ID: 101003469). The authors also acknowledge the support of the French Agence Nationale de la Recherche (ANR) under reference ANR-20-CE40-0025-01 (T-REX project), and the ANR-Melody.

APPENDIX

Proof Lemma 5.2. The proof of Lemma 5.2 we present next is based on telescopic sum arguments introduced in [28, 29] and popularized in [2].

Proof. For all $\epsilon > 0$, $\delta > 0$,

$$\begin{aligned} pr(S_n(\alpha) > x_n^\alpha) = &pr\big(S_n(\alpha) > x_n^\alpha,\, \textstyle\sum_{t=1}^n |X_t|^\alpha \mathbb{1}_{\{|X_t| \le \epsilon\, x_n\}} < \delta\, x_n^\alpha\big) \\ &+ pr\big(S_n(\alpha) > x_n^\alpha,\, \textstyle\sum_{t=1}^n |X_t|^\alpha \mathbb{1}_{\{|X_t| \le \epsilon\, x_n\}} > \delta\, x_n^\alpha\big). \end{aligned}$$

Referring to the vanishing-small-values condition in (20), the probability term above satisfies

$$\begin{aligned} pr\big(\textstyle\sum_{t=1}^n |X_t|^\alpha \mathbb{1}_{\{|X_t| > \epsilon\, x_n\}} > x_n^\alpha\big) \le pr(S_n(\alpha) > x_n^\alpha) \le \\ pr\big(\textstyle\sum_{t=1}^n |X_t|^\alpha \mathbb{1}_{\{|X_t| > \epsilon\, x_n\}} > (1-\delta) x_n^\alpha\big) + o(n\, pr(|X| > x_n)). \end{aligned}$$

Hence, to show (21) it suffices to prove that for all $\delta > 0$ the following relation holds

$$\lim_{\delta \to 0} \lim_{\epsilon \to 0} \lim_{n \to +\infty} \frac{pr\big(\sum_{t=1}^n |X_t|^\alpha \mathbb{1}_{\{|X_t| > \epsilon\, x_n\}} > (1-\delta) x_n^\alpha\big)}{n\, pr(|X| > x_n)} = 1. \tag{24}$$

Using the so-called telescopic sum argument, we see that the term in (24) satisfies

$$\begin{aligned} &pr\big(\textstyle\sum_{t=1}^n |X_t|^\alpha \mathbb{1}_{\{|X_t| > \epsilon\, x_n\}} > (1-\delta) x_n^\alpha\big) \\ &\quad = \textstyle\sum_{j=1}^{n-1} \Big\{ pr\big(\sum_{t=1}^{j+1} |X_t|^\alpha \mathbb{1}_{\{|X_t| > \epsilon\, x_n\}} > (1-\delta) x_n^\alpha\,,\, |X_1| > \epsilon\, x_n\big) \\ &\qquad - pr\big(\textstyle\sum_{t=2}^{j+1} |X_t|^\alpha \mathbb{1}_{\{|X_t| > \epsilon\, x_n\}} > (1-\delta) x_n^\alpha\,,\, |X_1| > \epsilon\, x_n\big) \Big\} \\ &\qquad + pr(|X_1|^\alpha > (1-\delta) x_n^\alpha). \end{aligned}$$

Then, by the anti-clustering condition in (18) we have that for all $K > 0$, the asymptotic approximation below

$$\begin{aligned} &pr\big(\textstyle\sum_{t=1}^n |X_t|^\alpha \mathbb{1}_{\{|X_t| > \epsilon\, x_n\}} > (1-\delta) x_n^\alpha\big) \\ &\quad = \textstyle\sum_{j=K}^{n-1} \Big\{ pr\big(\sum_{t=1}^{K} |X_t|^\alpha \mathbb{1}_{\{|X_t| > \epsilon\, x_n\}} > (1-\delta) x_n^\alpha\,,\, |X_1| > \epsilon\, x_n\big) \\ &\qquad - pr\big(\textstyle\sum_{t=2}^{K} |X_t|^\alpha \mathbb{1}_{\{|X_t| > \epsilon\, x_n\}} > (1-\delta) x_n^\alpha\,,\, |X_1| > \epsilon\, x_n\big) \Big\} \\ &\qquad + pr(|X_1|^\alpha > (1-\delta) x_n^\alpha) + o(n\, pr(|X| > x_n)). \end{aligned}$$

Putting everything together and using the limit in distribution from equation (5) we obtain the following asymptotic equivalence

$$\lim_{n\to+\infty} \frac{pr\big(\sum_{t=1}^{n}|X_t|^{\alpha}\mathbb{1}_{\{|X_t|>\epsilon\, x_n\}} > (1-\delta)x_n^{\alpha}\big)}{n\, pr(|X|>x_n)} = \lim_{\epsilon\downarrow 0}\lim_{K\to+\infty}\big\{\epsilon^{-\alpha}\int_1^{\infty} pr\big(\sum_{t=0}^{K}|\epsilon y\Theta_t|^{\alpha}\mathbb{1}_{\{y|\Theta_t|>1\}} > (1-\delta)\big) - pr\big(\sum_{t=1}^{K}|\epsilon y\Theta_t|^{\alpha}\mathbb{1}_{\{y|\Theta_t|>1\}} > (1-\delta)\big)d(-y^{-\alpha})\big\}.$$

This relation holds since the points of dicontinuity at the limit are contained in $\cup_{t=1}^{K}\{Y|\Theta_t|=1\}$, which has limit mass equal to zero.

Finally, by monotone convergence we can take the limit as $K\to+\infty$ within the integral. Furthermore, using the change of coordinates $u=\epsilon\, y$ we have that the term above is asymptotically equivalent to

$$\lim_{n\to+\infty} \frac{pr\big(\sum_{t=1}^{n}|X_t|^{\alpha}\mathbb{1}_{\{|X_t|>\epsilon\, x_n\}} > (1-\delta)x_n^{\alpha}\big)}{n\, pr(|X|>x_n)} = \lim_{\epsilon\downarrow 0}\big\{\int_{\epsilon}^{\infty} pr\big(\sum_{t=0}^{\infty}|y\Theta_t|^{\alpha}\mathbb{1}_{\{y|\Theta_t|>\epsilon\}} > (1-\delta)\big) - pr\Big(\sum_{t=1}^{\infty}|y\Theta_t|^{\alpha}\mathbb{1}_{\{y|\Theta_t|>\epsilon\}} > (1-\delta)\big)d(-y^{-\alpha})\big\}.$$

We conclude by monotone convergence that we can take the limit as ϵ goes to zero at each term.As a result we obtain asymptotic equivalence with the term below

$$\begin{aligned}&\sim \int_0^{\infty} pr\big(\textstyle\sum_{t=0}^{\infty}|y\Theta_t|^{\alpha} > (1-\delta)\big) - pr\big(\sum_{t=1}^{\infty}|y\Theta_t|^{\alpha} > (1-\delta)\big)d(-y^{-\alpha})\\ &= (1-\delta)^{-1}\mathbb{E}\big[\textstyle\sum_{t=0}^{\infty}|\Theta_t|^{\alpha} - \sum_{t=1}^{\infty}|\Theta_t|^{\alpha}\big]\\ &= (1-\delta)^{-1}.\end{aligned}$$

In the last step we use that $|\Theta_0|=1$. Finally, we conclude taking the limit as δ goes to zero that the relation 24 holds and this concludes the proof. □

Proof Theorem 5.3.

Proof. Let $(Z_t)_{t\in\mathbb{Z}}$ be an $\mathbb{R}^d$–valued regularly varying time series with index equal to one. We introduce the truncation notation where, for $\epsilon>0$, we denote $S_n := \sum_{t=1}^{n} Z_t$ and

$$\underline{S_n/c_n}_{\epsilon} := \textstyle\sum_{t=1}^{n} Z_t/c_n\mathbb{1}_{\{|Z_t|>\epsilon\, c_n\}}, \quad \overline{S_n/c_n}^{\epsilon} := \sum_{t=1}^{n} Z_t/c_n\mathbb{1}_{\{|Z_t|\le\epsilon\, c_n\}}.$$

We also consider a truncation of the centering sequence $(d_n)_{n\in\mathbb{N}}$ defined by

$$\underline{d_n/c_n}_{\epsilon} := \mathbb{E}[Z/c_n\mathbb{1}_{\{\epsilon\, c_n<|Z|\le c_n\}}], \quad n\in\mathbb{N}.$$

To simplify we denote the cluster process $(Q_t^Z)_{t\in\mathbb{Z}} := (Q_t)$. From the mixing condition in (22) we deduce there exists a sequence $k:=k_n\to+\infty$ such that, for all $u\in\mathbb{R}^d$,

$$\mathbb{E}\big[\exp\big\{i\,u\,(S_n/c_n - n\,d_n/c_n)\big\}\big] \sim \mathbb{E}\big[\exp\big\{i\,u\,(S_k/c_n - k\,d_n/c_n)\big\}\big]^{\lfloor n/k\rfloor}.$$

as $n \to +\infty$. Then, taking the logarithm at both sides yields

$$\begin{aligned}\log \mathbb{E}\big[\exp\big\{i\,u\,(S_n/c_n - n\,d_n/c_n)\big\}\big] &\sim \frac{n}{k}\log \mathbb{E}\big[\exp\big\{i\,u\,(S_k/c_n - k\,d_n/c_n)\big\}\big] \\ &\sim \frac{\mathbb{E}\big[\exp\big\{i\,u\,(S_k/c_n - k\,d_n/c_n)\big\}\big] - 1}{k\,pr(|Z| > c_n)} \\ &\sim \frac{\mathbb{E}\big[\exp\big\{i\,u\,(\underline{S_k/c_n}_\epsilon - k\,\underline{d_n/c_n}_\epsilon)\big\}\big] - 1}{k\,pr(|Z| > c_n)}.\end{aligned}$$

such that the second step is granted since $k\,d_n/c_n \to 0$ as $n \to +\infty$ and also $S_k/c_n \xrightarrow{\mathbb{P}} 0$ as $n \to +\infty$ and the last step follows by the vanishing-small-values condition in (20) and boundedness of the exponential function. Then, it follows from a Taylor expansion that

$$\begin{aligned}\Big|\big(\mathbb{E}\big[\exp\big\{i\,u\,(\underline{S_k/c_n}_\epsilon - k\,\underline{d_n/c_n}_\epsilon)\big\}\big] - 1\big) \\ - \big(\mathbb{E}\big[\exp\big\{i\,u\,\underline{S_k/c_n}_\epsilon\big\}\big] - 1 - i\mathbb{E}[\sin(u\,\overline{\underline{S_k/c_n}_\epsilon}^{1})]\big)\Big| \\ = O\big(k\,\underline{d_n/c_n}_\epsilon\,\mathbb{E}[|\underline{S_k/c_n}_\epsilon|\mathbb{1}(|\underline{S_k/c_n}_\epsilon| \le 1)]\big).\end{aligned}$$

Moreover, $|k\,\underline{d_n/c_n}_\epsilon\,\mathbb{E}[|\underline{S_k/c_n}_\epsilon|\mathbb{1}(|\underline{S_k/c_n}_\epsilon| \le 1)]|/k\,pr(|X| > a_n) \to 0$ as $n \to +\infty$. Thus, we obtain the asymptotic equivalence

$$\begin{aligned}&\log \mathbb{E}\big[\exp\big\{i\,u\,(\underline{S_n(\alpha)/c_n}_\epsilon - n\,\underline{d_n/c_n}_\epsilon)\big\}\big] \\ &\sim \frac{\mathbb{E}\big[\exp\big\{i\,u\,\underline{S_k/c_n}_\epsilon\big\} - 1 - i\sin(u\,\overline{\underline{S_k/c_n}_\epsilon}^{1})\big]}{k\,pr(|Z| > c_n)}.\end{aligned}$$

as $n \to +\infty$. Furthermore,

$$\begin{aligned}&\mathbb{E}\big[\exp\big\{i\,u\,\underline{S_k/c_n}_\epsilon\big\} - 1 - i\sin(u\,\overline{\underline{S_k/c_n}_\epsilon}^{1})\big] \\ &= \mathbb{E}\big[\big(\exp\big\{i\,u\,\underline{S_k/c_n}_\epsilon\big\} - 1\big)\mathbb{1}_{\{S_k > \epsilon\,c_n\}}\big] - \mathbb{E}\big[i\sin(u\,\overline{\underline{S_k/c_n}_\epsilon}^{1})\mathbb{1}_{\{S_k > \epsilon\,c_n\}}\big].\end{aligned}$$

For all $x \in \mathbb{R}$, we denote $x\mathbb{1}_{|x|>\epsilon}$ by $\underline{x}_\epsilon$, and similarly we denote $x\mathbb{1}_{|x|\le 1}$ by $\overline{x}^1$. Then, conditioning to the event $\{S_k > \epsilon\,c_n\}$, we use the limit relation in (21) and Proposition 4.2. in [7] and take the limit as n goes to infinity in the above expression. Hence,

$$\begin{aligned}&\frac{\mathbb{E}\big[\exp\big\{i\,u\underline{S_k/c_n}_\epsilon\big\} - 1 - i\sin(u\,\overline{\underline{S_k/c_n}_\epsilon}^{1})\big]}{kpr(|X| > a_n)} \\ &\sim \int_0^\infty \mathbb{E}\big[\exp\big\{it\sum_{t\in\mathbb{Z}}\underline{yQ_t}_\epsilon\big\} - 1 - i\sin\big(u\sum_{t\in\mathbb{Z}}(\overline{\underline{yQ_t}_\epsilon}^{1})\big]\,d(-y^{-1}),\end{aligned}$$

where $(Q_t)_{t\in\mathbb{Z}}$ is the cluster process of the stationary process (Z_t). In particular, it takes values in $\mathbb{R}^{\mathbb{Z}}$ and verifies $\sum_{t\in\mathbb{Z}}|Q_t| = 1$ with probability one.

Let $\delta > 0$ and let's divide the integral above on the events $\{y > \delta\}$ and $\{y \leq \delta\}$. Over the event $\{y \leq \delta\}$ we have that given we choose $\delta < 1$,

$$\begin{aligned}&\int_0^\infty \mathbb{E}\big[\exp\big\{iu\textstyle\sum_{t\in\mathbb{Z}}\underline{yQ_t}_\epsilon\big\} - 1 - i\sin\big(u\textstyle\sum_{t\in\mathbb{Z}}\overline{\underline{yQ_t}_\epsilon}^{-1}\big)\big]\mathbb{1}(y\leq\delta)\,d(-y^{-1})\\ &= \int_0^\infty \mathbb{E}\big[\exp\big\{iu\textstyle\sum_{t\in\mathbb{Z}}\underline{yQ_t}_\epsilon\big\} - 1 - i\sin\big(u\textstyle\sum_{t\in\mathbb{Z}}\underline{yQ_t}_\epsilon\big)\big]\mathbb{1}(y\leq\delta)\,d(-y^{-1}).\end{aligned}$$

Then, using the inequality $|\exp\{iz\} - 1 - i\sin(z)| \leq |z|^2$ for all $z \in \mathbb{R}$, the integral above is bounded in absolute value by

$$\int_0^\infty \mathbb{E}\big[\big|u\textstyle\sum_{t\in\mathbb{Z}}|yQ_t|\big|^2\big]\mathbb{1}(y\leq\delta)d(-y^{-1}) \leq \delta\mathbb{E}\big[\big|u\textstyle\sum_{t\in\mathbb{Z}}|Q_t|\big|^2\big] = \delta u^2 < +\infty.$$

Then, we conclude that

$$\begin{aligned}&\log\mathbb{E}\big[\exp\big\{i\,u\,(S_k/c_n - n\,d_n/c_n)\big\}\big]\\ &\sim \lim_{\delta\to 0}\int_\delta^\infty \mathbb{E}\big[\exp\big\{i\,u\textstyle\sum_{t\in\mathbb{Z}}yQ_t\big\} - 1 - i\sin\big(u\textstyle\sum_{t\in\mathbb{Z}}\overline{yQ_t}^{-1}\big)\big]d(-y^{-1}).\end{aligned}$$

Moreover, we can rewrite the term above as the sum of two integrals as shown below

$$\begin{aligned}&\lim_{\delta\to 0}\int_\delta^\infty \mathbb{E}\big[\exp\big\{i\,u\textstyle\sum_{t\in\mathbb{Z}}yQ_t\big\} - 1 - i\sin\big(u\textstyle\sum_{t\in\mathbb{Z}}yQ_t\big)\big]d(-y^{-1})\\ &\quad + i\int_1^\infty \mathbb{E}\big[\sin\big(u\textstyle\sum_{t\in\mathbb{Z}}yQ_t\big) - \sin\big(u\textstyle\sum_{t\in\mathbb{Z}}yQ_t - u\textstyle\sum_{t\in\mathbb{Z}}\underline{yQ_t}_1\big)\big]d(-y^{-1})\\ &= I + II\end{aligned}$$

such that the for the last term we can use the trigonometric relation

$$\sin(p) - \sin(p-q) = 2\sin(p/2)\cos(p-(q/2))$$

for $p, q \in \mathbb{R}$, to obtain that the second term II is bounded in absolute value by $\int_1^{+\infty} y^{-2} = 1$. This term can be interpreted as a location parameter.

Finally, by monotone convergence, using the bound previously derived, we can take the limit as δ goes to 0 and we conclude that

$$\begin{aligned}&\log\mathbb{E}\big[\exp\big\{i\,u\,(S_k/c_n - n\,d_n/c_n)\big\}\big]\\ &\quad\sim \int_0^\infty \mathbb{E}\big[\exp\big\{i\,u\textstyle\sum_{t\in\mathbb{Z}}yQ_t\big\} - 1 - i\sin\big(u\textstyle\sum_{t\in\mathbb{Z}}yQ_t\big)\big]d(-y^{-1})\\ &\qquad + i\int_1^\infty \mathbb{E}\big[\sin\big(u\textstyle\sum_{t\in\mathbb{Z}}yQ_t\big) - \sin\big(u\textstyle\sum_{t\in\mathbb{Z}}yQ_t - u\textstyle\sum_{t\in\mathbb{Z}}\underline{yQ_t}_1\big)\big]d(-y^{-1}).\end{aligned}$$

as $n \to +\infty$. We have shown that the limit relation from equation (23) holds and this concludes the proof. □

REFERENCES

[1] P. Asadi, S. Engelke, and A. C. Davison. Optimal regionalization of extreme value distributions for flood estimation. *Journal of Hydrology*, 556:182–193, 2018.

[2] K. Bartkiewicz, A. Jakubowski, T. Mikosch, and O. Wintenberger. Stable limits for sums of dependent infinite variance random variables. *Probability theory and related fields*, 150:337–372, 2011.

[3] B. Basrak, H. Planini, and P. Soulier. An invariance principle for sums and record times of regularly varying stationary sequences. *Probability Theory and Related Fields*, 172:869–914, 2018.

[4] B. Basrak and J. Segers. Regularly varying time series. *Stoch. Proc. Appl.*, 119:1055–1080, 2009.

[5] D. Buraczewski, E. Damek, T. Mikosch, and J. Zienkiewicz. Large deviations for solutions to stochastic recurrence equations under kesten's conditions. *The annals of Probability*, 41:2755–2790, 2013.

[6] G. Buriticá, N. Meyer, T. Mikosch, and O. Wintenberger. Some variations on the extremal index. *Zap. Nauchn. Semin. POMI.*, 30:52–77, 2021. To be translated in J.Math.Sci. (Springer).

[7] G. Buriticá, T. Mikosch, and O. Wintenberger. Threshold selection for cluster inference based on large deviation principles. 2021. arXiv preprint arXiv:2106.12822.

[8] B. Coles, J. Bawa, L. Trenner, and P. Dorazio. *An introduction to statistical modeling of extreme values*. Springer, London, 2001.

[9] D. Cooley, R. A. Davis, and P. Naveau. Approximating the conditional density given large observed values via a multivariate extremes framework, with application to environmental data. *Annals of Applied Statistics*, 6(4):1406–1429, 2012.

[10] R. A. Davis, H. Drees, J. Segers, and M. Warchol. Inference on the tail process with application to financial time series modeling. *Journal of Econometrics*, 205:508–525, 2018.

[11] R. A. Davis and T. Hsing. Point process and partial sum convergence of weakly dependent random variables with infinite variance. *The Annals of Probability*, 23:879–917, 1995.

[12] R. A. Davis and T. Mikosch. The extremogram: A correlogram for extreme events. *Bernoulli*, 15(4):977–1009, 2009.

[13] L. de Haan, G. Mercadier, and C. Zhou. Adapting extreme value statistics to financial time series: dealing wih bias and serial dependence. *Finance and Stochastics*, 20:321–354, 2016.

[14] H. Drees, A. Janssen, and S. Neblung. Cluster based inference for extremes of time series. 2021. ArXiv preprint arXiv:2103.08512.

[15] W. H. DuMouchel. *Stable distributions in Statistical inference*. PhD thesis, Yale University, 1971.

[16] W. H. Dumouchel. On the asymptotic normality of the maximum-likelihood estimate when sampling from a stable distrbibution. *The annals of Statistics*, 1:948–957, 1973a.

[17] W. H. Dumouchel. Stable distributions in statistical inference 1: Symmetric stable distributions compared to other symmetric long-tailed distributions. *JASA*, 68:469–477, 1973b.

[18] W. H. Dumouchel. Stable distributions in statistical inference 2: Information from stable distributed sampled. *JASA*, 40:386–393, 1975.

[19] P. Embrechts, C. Kluppelberg, and T. Mikosch. *Modelling extremal events: for insurance and finance*, volume 13. Springer, Zurich, 2013.

[20] G. Evin, A.C. Favre, and B. Hingray. Stochastic generation of multi-site daily precipitation focusing on extreme events. *Hydrology and Earth System Sciences*, 22(1):655–672, 2018.

[21] W. Feller. *An introduction to probability theory and its applications*, volume 2. John Wiley & Sons, New York, 2008.
[22] M. Ferreira and H. Ferreira. Extremes of multivariate armax processes. *TEST: An. oofícial Journal of Spanish Society of Statistics and Operations Research*, 22:606–627, 2013.
[23] C. A. Ferro and J. Segers. Inference for clusters of extreme values. *Journal of the royal Statistical Society: Series B (statistical Methodology)*, 65:545–556, 2003.
[24] E. Gilleland and R. W. Katz. extremes 2.0: An extreme value analysis package in r. *Journal of Statistical Software*, 27:1–39, 2016.
[25] M. I. Gomes, L. de Haan, and L. Peng. Semi-parametric estimation of the second order parameter in statistics of extremes. *Extremes*, 5:387–414, 2002.
[26] R. Huser and J. L. Wadsworth. Advances in statistical modeling of spatial extremes. *Wiley Interdisciplinary Reviews: Computational Statistics*, page e1537, 2020.
[27] IPCC. *Climate Change 2021: The Physical Science Basis. Contribution of Working Group I to the Sixth Assessment Report of the Intergovernmental Panel on Climate Change*. Cambridge University Press (In Press), 2021.
[28] A. Jakubowski. Minimal conditions in p–stable limit theorems. *Stochastic processes and their applocations*, 44:291–327, 1993.
[29] A. Jakubowski. Minimal conditions in p–stable limit theorems – ii. *Stochastic processes and their applications*, 68:1–20, 1997.
[30] V. V. Kharin, F. W. Zwiers X. Zhang, and M. Wehner. Changes in temperature and precipitation extremes in the cmip5 ensemble. *Climatic change*, 119(2):345–357, 2013.
[31] D. G. Konstantinides and T. Mikosch. Large deviations and ruin probabilities for soutions to stochastic recurrence equations with heavy-tailed innovations. *The Annals of Probability*, 33:1992–2035, 2005.
[32] R. Kulik and P. Soulier. *Heavy-tailed time series*. Springer, 2020.
[33] M. R. Leadbetter. Extremes and local dependence in stationary sequences. *Probability Theory and Related Fields*, 65:291–306, 1983.
[34] M. R. Leadbetter, G. Lindreg, and H. Rootzen. *Extremes and Related Properties of Random Sequences and Processes*. Springer, Berlin, 1983.
[35] T. Mikosch and G. Samorodnitsky. The supremum of a negative drift random walk with dependent heavy-tailed steps. *The Annals of Applied Probability*, 10:1025–1064, 2000.
[36] T. Mikosch and O. Wintenberger. Precise large deviations for dependent regularly varying sequences. *Probability Theory and Related Fields*, 156:851–887, 2013.
[37] J. P. Nolan. *Lévy processes: Theory and applications*, chapter Maximum likelihood estimation and diagnostics for stable distributions. Springer, Boston, 2001.
[38] J. P. Nolan. *Univariate stable distributions*. Springer, New York, 2020.

[39] G. Samorodnitsky, M. S. Taquu, and R. W. Linde. Stable non-gaussian random processes: stochastic models with infinite variance. *Bulletin of the London Mathematical Society*, 28:554–555, 1996.

[40] P. Tencaliec, A. C. Favre, P. Naveau, C. Prieur, and G. Nicolet. Flexible semiparametric generalized Pareto modeling of the entire range of rainfall amount. *Environmetrics*, https://doi.org/10.1002/env.2582:1–20, 2019.

[41] G. Toulemonde, A. Guillou, and P. Naveau. Particle filtering for gumbel distributed daily maxima of methane and nitrous oxide. *Environmetrics*, 24:51–62, 2013.

[42] J. Zscheischler, P. Naveau, O. Martius, S. Engelke, and C. C. Raible. Evaluating the dependence structure of compound precipitation and wind speed extremes. *Earth System Dynamics Discussions*, 2020:1–23, 2020.

LABORATOIRE DE PROBABILITÉS, STATISTIQUES ET MODÉLISATION, SORBONNE UNIVERSITÉ, 75005, PARIS, FRANCE

Email address: gloria.buritica@sorbonne-universite.fr

LABORATOIRE DE SCIENCES DU CLIMAT ET DE L'ENVIRONNEMENT, ESTIMR, IPSL-CNRS, 91191, GIF-SUR-YVETTE, FRANCE

Email address: philippe.naveau@lsce.ipsl.fr